Functional properties of the alternative NADH:ubiquinone oxidoreductase from *E. coli* through comparative 3-D modelling

Ralf Schmid, Dietlind L. Gerloff *

Biocomputing Research Unit, School of Biology, University of Edinburgh, Edinburgh, EH9 3JR, UK

Received 15 September 2004; revised 28 October 2004; accepted 31 October 2004

Available online 16 November 2004

Edited by Stuart Ferguson

Abstract The alternative NADH:ubiquinone oxidoreductase (NDH-2) from *Escherichia coli* is a membrane protein playing a prominent role in respiration by linking the reduction of NADH to the quinone pool. Remote sequence similarity reveals an evolutionary relation between alternative NADH:quinone oxidoreductases and the SCOP-family "FAD/NAD-linked reductases". We have created a structural model for NDH-2 from *E. coli* through comparative modelling onto a template from this family. Combined analysis of our model and sequence conservation allowed us to include the cofactor FAD and the substrate NADH in atomic detail. Furthermore, we propose the most plausible orientation of NDH-2 relative to the membrane and specify a region of the protein potentially involved in ubiquinone binding.

Keywords: NADH:ubiquinone oxidoreductase; NDH-2; Homology modelling; Membrane protein

1. Introduction

NADH is the central source of electrons in mitochondrial and bacterial respiration. Two major classes of NADH:quinone oxidoreductases link the oxidation of NADH to the reduction of ubiquinone or menaquinone in the mitochondrial or inner bacterial membrane. Respiratory complex I in mitochondria and related complexes in bacterial membranes (NDH-1) couple the oxidation of NADH with proton transfer across the membrane, and hence generate a proton motive force that is utilised for the synthesis of ATP. NDH-1 is a multisubunit protein complex bearing one flavin mononucleotide (FMN) and a series of Fe–S clusters as cofactors. In contrast, alternative NADH:quinone oxidoreductases (NDH-2) are not capable of translocating protons and only a single (≈45 kDa) protein has been associated with this reaction. NDH-2 catalyses electron transfer from NADH via FAD to ubiquinone and displays remote sequence similarity to proteins classified as "FAD/NAD-linked reductases" [1] in the Structural Classification of Proteins (SCOP) database (http://scop.mrc-lmb.cam.ac.uk/scop/). SCOP is curated by experts and provides a detailed and comprehensive classification of known protein structures based on their resemblance and evolutionary considerations [1]. All members of the SCOP-family "FAD/NAD-linked reductases" have the electron donator NAD(P)H and the cofactor FAD in common, while the final electron acceptor varies. The similarities in sequence and function suggest homology modelling as a suitable approach for elucidating the structural aspects of NDH-2 activity. Structural conservation between related proteins is particularly high within active sites, so information regarding enzymatic function can often be extracted from homology models even if sequence identity between template and target is low overall (<25%).

NDH-2 type enzymes have been found in mitochondria from primarily plant and fungal species, and in many bacteria. So far no tertiary structural information for any of these enzymes is available. Various species accomplishing respiration with NADH as electron source use either NDH-1, NDH-2 or both (see [2] for a review). *E. coli* expresses predominantly the respiratory complex I homologue NDH-1 under anoxygenic conditions, whereas under oxygenic conditions NDH-2 is significantly more abundant [3]. While NDH-2 from *E. coli* is one of the best studied alternative NADH:ubiquinone oxidoreductases little detail is known of the substrate and cofactor binding sites and the interaction between protein and membrane is a matter of dispute.

2. Methods

2.1. Fold recognition and sequence alignments

The amino acid sequence of *E. coli* NDH-2 (SWISS-PROT entry: DHNA_ECOLI) was submitted to the 3D-PSSM [4] (http://www.sbg.bio.ic.uk/servers/3dpssm/) and SAMT02 [5] (http://www.cse.ucsc.edu/research/compbio/HMM-apps/T02-query.html) www-servers for fold recognition, secondary structure prediction and preliminary sequence alignments. Further homologous sequences to DHNA_ECOLI and potential templates were retrieved using BLAST and PSI-BLAST [6] against the non-redundant and SWISS-PROT databases via the NPS@ www-server (http://npsa-pbil.ibcp.fr) [7]. Multiple alignments were generated using T-Coffee [8] and subsequently subjected to minor manual editing. A sequence alignment of "FAD/NAD-linked reductases" based on structural superposition of available 3D structures was produced using pairwise alignments by the CE www-server (http://cl.sdsc.edu/ce.html) [9]. Sequence alignments are provided as Supplemental Materials.

2.2. Homology modelling and data analysis

After careful examination of potential templates the structure of NADH-peroxidase from *Enterococcus faecalis* (PDB entry: 2NPX) [10] was chosen for modelling. A pairwise alignment between

*Corresponding author. Fax: +44 131 6507055.
E-mail address: d.gerloff@ed.ac.uk (D.L. Gerloff).

[1] FAD/NAD-linked reductases consist of the SCOP-domains c.3.1.5 (FAD/NAD-linked reductases, N-terminal and central domains) and d.87.1.1 (FAD/NAD-linked reductases, C-terminal domain).

Abbreviations: NDH-1, respiratory complex I; NDH-2, alternative NADH:ubiquinone oxidoreductase; TM, transmembrane; PDB, protein data bank; SCOP, structural classification of proteins data base; rmsd, root mean square deviation

0014-5793/$22.00
doi:10.1016/j.febslet.2004.10.093

NDH-2 from *E. coli* and the template sequence was manually adjusted taking into consideration multiple sequence alignments, structural alignments and the continuity of secondary structure elements. Series of 20 models for alternative plausible alignments were built using MODELLER 6v2 [11] with added restraints based on predicted secondary structure (elongating α-helices Pro143–Ser161, Ala179–Lys201 and Ala330–Met348 by 7, 10 and 4 residues, respectively). The highest ranking five models in each series were submitted to the WHATCHECK www-server (http://www.cmbi.kun.nl/WIWIWI/gv/servers/) [12] and inspected manually. Non-identical side chains between template and target were optimised using SCWRL [13], except if directly involved in binding FAD or NADH. Loop modelling and energy minimization (Tripos forcefield, 10 steps steepest descent followed by 100 steps conjugate gradient) was carried out in SYBYL 6.8 (Tripos Associates, St. Louis). For the prediction of transmembrane (TM) helices the NDH-2 sequence was submitted to the following servers: TMHMM [14], PHDTM [15], HMMTOP [16], TM-Pred [17], DAS [18], PRED-TMR [19], TM-Finder [20], TMAP [21], ALOM2 [22] and SOSUI [23]. Electrostatic surface calculations were performed using GRASP [24].

3. Results and discussion

3.1. NDH-2 belongs to the SCOP-family "FAD/NAD-linked reductases"

Fold recognition reveals unambiguously that NDH-2 is a member of the SCOP-family "FAD/NAD-linked reductases". All relevant hits retrieved from searching 3D-PSSM and SAMT02 with DHNA_ECOLI belong to this family, with *E*-values [2] as low as 0.00045 for 3D-PSSM (>95% certainty according to the web-page), and 5×10^{-43} for SAMT02. The SCOP-family "FAD/NAD-linked reductases" includes 11 functional subfamilies to date. All proteins within the family facilitate electron transfer reactions from NAD(P)H via the non-covalently bound cofactor FAD to electron acceptors that vary for each subfamily (e.g. H_2O_2, ferredoxin, glutathione), which suggests that NDH-2 is part of a new subfamily. In contrast to the membrane-bound NDH-2, all structurally characterised FAD/NAD-linked reductases are soluble enzymes, most of them forming homodimers. Each monomer consists of three domains. The most characteristic feature of the family is a structural motif consisting of 5 parallel β-strands topped by 3 anti-parallel β-strands which occurs in both the FAD and NADH-binding domains. The C-terminal dimerisation domain is the most divergent part amongst the functional subfamilies.

Manual inspection of possible templates from the "FAD/NAD-linked reductases" family (see Section 2) suggested the NADH-peroxidase from *Enterococcus faecalis* (SWISS-PROT entry: NAPE_ENTFA) as the most suitable template for modelling NDH-2. This is supported by a PSI-BLAST [6] search with DHNA_ECOLI as query sequence against SWISS-PROT hitting NAPE_ENTFA in iteration 2 with a score of 151 (*E*-value 4×10^{-36}). Eight structures for NAPE_ENTFA have been deposited in the PDB to date. Out of these we chose PDB-entry 2NPX as the only wild-type structure including a bound NADH substrate [10].

The most crucial step in homology modelling at low (<25%) sequence identity is the alignment between target and template. Information extracted from multiple alignments of both the template and target subfamilies as well as structural alignments was used to place insertions and deletions. Secondary structure elements were kept uninterrupted and exposed sites were selected for insertions into the template structure. Ignoring gaps in the threading alignment DHNA_ECOLI and NAPE_ENTFA share 21% sequence identity; a further 25% of the aligned positions are conservative substitutions.

3.2. A control model confirms the suitability of the approach for modelling NDH-2

The structure of NAPE_ENTFA (PDB-entry: 2NPX) was modelled based on the structure of lipoamide dehydrogenase from *Pseudomonas putida* (PDB-entry: 1LVL) using the same approach as for modelling NDH-2. The sequence identity between 2NPX and 1LVL is 23%, a further 21% are conservative changes. This control experiment allows us to evaluate the modelling procedure and hence, to estimate the reliability of the NDH-2 model at different levels of detail. The rmsd between the control model and the corresponding experimentally determined structure 2NPX was 2.84 Å over C_α atoms in the N-terminal domain (residues 1–321) and 3.18 Å over the C-terminal domain (residues 322–444). Excluding four loop insertions with respect to the template (residues 134–138, 145–148, 284–295 and 425–431) improves the rmsd to 2.38 Å (N-terminal domain) and to 2.29 Å (C-terminal domain), respectively. For 17 out of the 18 residues within contact distance to FAD (<3.5 Å) an excellent 0.81 Å rmsd over all atoms (including side chains) was attained. Putative hydrogen bonds were determined using the LPC www-server (http://bip.weizmann.ac.il/oca-bin/lpccsu) with a distance cut-off of 3.3 Å [25]. Of the 16 putative hydrogen bonds between protein and FAD that are present in the 2NPX structure, 14 were also detected in the control model. The electrostatic surfaces of the experimentally determined structure and the control model revealed no major differences but were visibly different from that of the template, 1LVL (data not shown). These results demonstrate that our approach is sufficiently accurate to yield a realistic impression of the NDH-2 structure overall, a model of the FAD and NADH binding sites in atomic detail, and electrostatic surfaces at a resolution allowing qualitative interpretation.

3.3. The model of NDH-2 reveals details of the FAD, NADH and putative ubiquinone and Cu(I) binding sites

Our final model for NDH-2 comprises 385 amino acid residues, the cofactor FAD and the substrate NADH. Both the FAD and the NADH-binding domains show the characteristic structural motif (see Section 3.1) and the redox active parts of the cofactors (i.e. the nicotinamide ring of NADH and the isoalloxazine ring of FADH) are orientated in parallel, in close proximity of each other (<3 Å), to facilitate electron transfer (see Fig. 1). Most residues involved in cofactor binding belong to established "sequence fingerprints" [26,27] and are amongst the most highly conserved residues within the sequence alignments. Since our evaluation suggests that the model of NDH-2 is most accurate in these areas we are confident that the 10 hydrogen bonds found involved in FAD binding, and the 8 hydrogen bonds to NADH, are a reasonable approximation of the hydrogen bonding pattern in the actual sites (see Fig. 2 for details).

The 48 C-terminal residues of NDH-2 could not be modelled in detail due to ambiguities in the alignment. In all so far known FAD/NAD-linked reductases the C-terminal domain is responsible for dimerisation. Since NDH-2 has not been shown to form a functional dimer, it is perhaps not surprising

[2] *E*-value = probability of a random hit

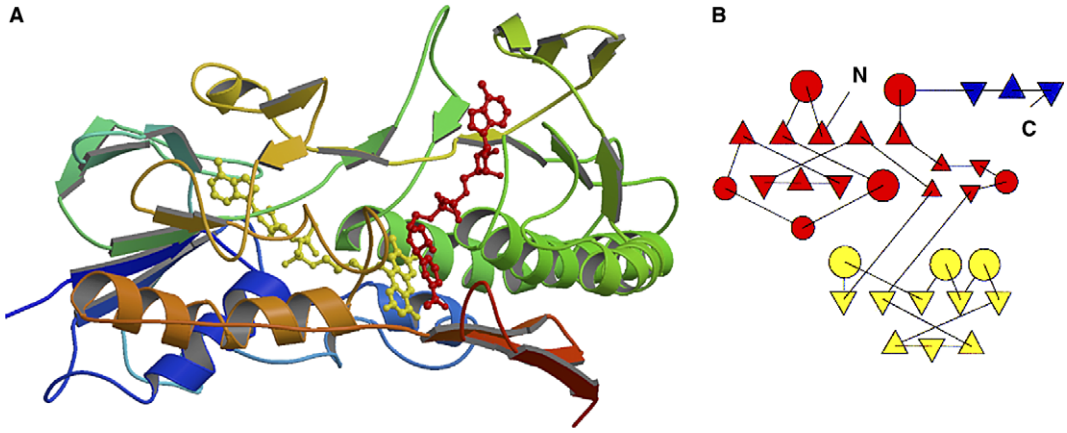

Fig. 1. (A) Ribbon representation of modelled alternative NADH:ubiquinone dehydrogenase from *E. coli* (NDH-2). The ribbon is colour-coded from N-terminus (blue) to C-terminus (red). FAD and NADH are displayed as ball and stick models coloured in yellow and red, respectively. The residue identified as potentially involved in quinone binding, His51, forms part of the light blue helix behind the FAD molecule (not shown). The diagram was created using MOLSCRIPT [43] and RASTER3D [44]. (B) TOPS-Topology cartoon [45] of the model. Circles and triangles represent α-helices and β-strands, respectively. The FAD-domain (Thr1–Asn129, Gly274–Gly350), NADH-domain (Thr130–Ala273) and the C-terminal domain (Lys351–Met385) are coloured in red, yellow and blue, respectively.

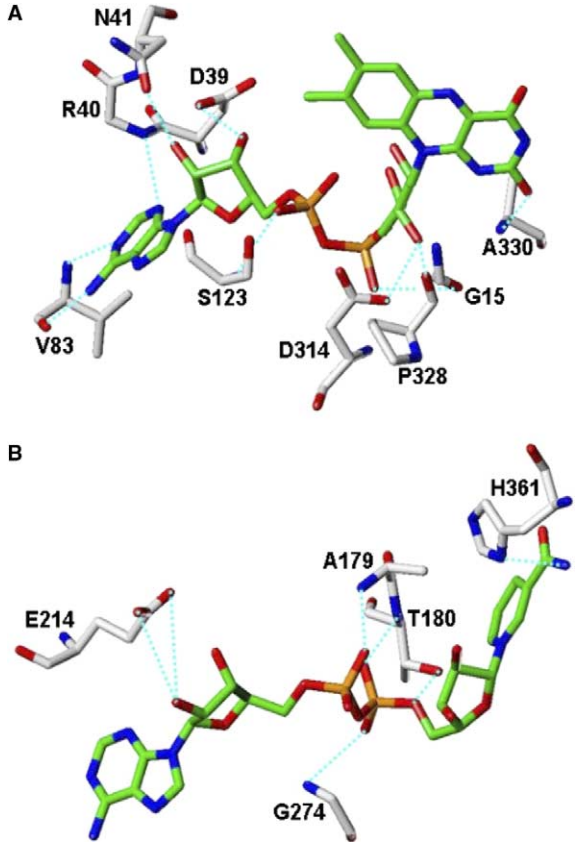

Fig. 2. Detailed views of the FAD binding site (A) and the NADH binding site (B). Displayed are all protein residues within 3.3 Å of FAD or NADH that are likely to be involved in hydrogen bonding to these cofactors. Atoms are coloured according to CPK (carbon-white; oxygen-red; nitrogen-blue; phosphorous-orange), carbon atoms in FAD and NADH are depicted in green for better distinction. The side chain of Arg40 was omitted for clarity. Predicted hydrogen bonds between protein and FAD or NADH are indicated by dotted lines. The figure was produced using SYBYL 6.8 (Tripos Associates, St. Louis).

that the structure of this domain should differ significantly from the template. A possible role for these residues, derived from secondary structure prediction and sequence analysis is discussed in Section 3.4.

It is assumed that all FAD/NAD-linked reductases have evolved from a common ancestor, but acquired their ability to react with their respective electron acceptors independently [28]. Indeed, the variety of electron acceptors used is reflected in the only marginal overall sequence conservation throughout the family at the relevant site. However, subfamily specific sequence conservation is found instead (Supplemental Material). For example, Cys42 as the oxygen transferring residue in the active site of 2NPX is entirely conserved within the subfamily of NADH-(per)oxidases. In contrast to the FAD and NADH binding sites details of the ubiquinone binding site, such as which residues are involved in hydrogen bonding, cannot be derived from the structural model directly. Instead, deriving information about the NDH-2 ubiquinone binding site must rely on combined analysis of evolutionary information (such as sequence conservation within the NDH-2 subfamily), physical restraints (such as distance dependence of the probability for successful electron transfer events), and the structural information obtained from homology modelling. To achieve efficient electron transfer the electron acceptor, (ubiquinone in the case of NDH-2 and H_2O_2 for 2NPX) has to be in close proximity of the cofactor FAD. For example, the acceptor site in 2NPX is in close contact to the isoalloxazin ring of the FAD molecule and the residues most crucial for catalysis are located between strand 2 and strand 3 of the N-terminal 5-stranded β-sheet. This provides an ideal arrangement for efficient electron transfer from NADH via FAD to H_2O_2. Similarily, we expect the ubiquinone binding site in NDH-2 close to the FAD and the isoalloxazin ring of FAD "sandwiched" between the nicotinamide of NADH and ubiquinone. Ubiquinone is a lipid-like, hydrophobic compound present primarily in the membrane, therefore its binding site on NDH-2 would also be expected close to the membrane. Together this points particularly to the region between

Ser43 and Gly75 for ubiquinone binding and sequence conservation in the NDH-2 subfamily reveals His51 (His or Tyr in the bacterial NDH-2 in the alignment) as a potential hydrogen bond donator for ubiquinone at <5 Å distance from the FAD-isoalloxazine in our model. One could argue that this suggestion is supported, to an extent, by weak similarity in the sequence alignment to a consensus sequence pattern L–X(3)–H–X(3)–(S/T) at known quinone binding sites described by Fisher et al. [29]. However, these local similarities are clearly too weak to be significant and the more recently solved structures of membrane proteins with quinone binding sites have discouraged the idea of such a simple sequence motif for quinone binding. Instead they encourage the idea that subfamily conserved residues may be involved in hydrogen bonding and proton shuttling [30]. It is worthwhile mentioning that an ubiquinone site in close contact to FAD, as is proposed here for NDH-2, is reminiscent of the unspecific quinone binding site in the soluble NAD(P)H:quinone oxidoreductase which resembles the flavodoxin fold [31].

A conserved Trypthophan residue (Trp271 in *E. coli* NDH-2) has previously been suggested to be engaged in a π-stacking interaction with the quinone ring [32]. Our model shows that Trp271 is part of a sequence stretch interacting with the adenosine moiety of NADH. With its aromatic side chain within 6 Å distance from the adenine ring, as compared to >15 Å to the redox active nicotinamide of NADH and isoalloxazin of FAD, we conclude that this residue is not involved in quinone binding, but part of the hydrophobic pocket binding the NADH-adenine.

Recently, the reduction of Cu(II) was reported as an additional function of NDH-2 [33], and a putative Cu(I) binding site formed mainly by Cys315 and Cys318, with Cys137, His334 or Cys339 as potential additional ligands, was postulated [34]. To test this hypothesis, we built an additional NDH-2 model using distance restraints to force the sulphur atoms of Cys315 and Cys318 into a distance suitable for coordination of a Cu(I)-ion without finding major distortions of the overall fold. Assuming that Cys315 and Cys318 are indeed part of a Cu(I) binding site, Cys137 is unlikely to also be involved since it is >25 Å away. His334 and Cys339 are part of a helix (Ala330–Asn349) which extends along the putative Cu(I) binding site, but neither is pointing towards it. While the possibility of an induced conformational change upon metal binding cannot be ruled out entirely and could potentially modify the availability of Cys137 for coordination, the orientation of this helix is unambiguously determined by the positions of the highly conserved Ala330 and Ala333 which are facing the flavin part of FAD and are part of its binding site. Based on our model Met336 and Lys354 (assuming an uncharged lysine side chain) would make more plausible additional ligands of Cu(I). However, there is no obvious conserved "fingerprint" in the sequence alignment that would link Cys315, Cys318, Met336 and/or Lys354. In the absence of further experimental evidence, the lack of a noticeable conservation pattern at any of the positions including candidates for its coordination must be taken to suggest that Cu(I) binding is a feature limited to, at best, the closest homologues of *E. coli* NDH-2.

3.4. Membrane interaction of NDH-2 seems to be mediated by amphipathic helices and electrostatic interactions

Membrane binding is a unique feature of the NDH-subfamily within the "FAD/NAD-linked reductases" SCOP-family. In general, protein binding to membranes is mediated by hydrophobic interactions (e.g. through transmembrane helices) and electrostatic interactions (mainly between positively charged protein residues and negatively charged phosphatidyl groups on the membrane surface). Recently, improvements in TM- and membrane topology prediction have been reported when consensus predictions were based on several methods [35]. Accordingly we submitted the NDH-2 sequence to 10 different TM-prediction servers and analysed the results. Five methods (TMHMM [14], PRED-TMR [19], TMAP [21], ALOM2 [22], SOSUI [23]) predicted no TM-helices at all. DAS [18] predicted only short (<8 residues) TM-regions which are unlikely to form membrane spanning helices. PHDTM [15], TMPred [17], TM-Finder [20], and HMMTOP [16] predicted one, or several, TM-helices at the C-terminus, but these methods produce a higher proportion of false positive results (typically from 11% HMMTOP to 55% TMPred by contrast to <2% TMHMM [36]). Automated secondary structure prediction for this region predicts one long, or two shorter, α-helices between Ile393 and Ile422. A more thorough analysis of sequence conservation and topology as described in [37] suggests the presence of two helices (Arg390–Ala406, Gly409–Arg424), both displaying amphipathic properties as is typical for helices on the protein surface (Fig. 3). The preference for positively charged residues on the hydrophilic side of these predicted helices, in combination with the relatively high abundance of tryptophan and tyrosine residues which are known to be important for membrane binding [38], makes them likely candidate sites of interaction with the phosphatidyl groups of the membrane. Our analysis cannot completely rule out the possibility of a single C-terminal TM-helix but this would place His408–Tyr410 in *E. coli* NDH-2 in its centre, while these residues are matched by a stretch of three charged/polar residues in several other members of the NDH-2 subfamily (for details see Supplemental Material). Contrary to proteins with multiple TM-helices NDH-2 could not compensate for such charges through inter-TM-helix salt bridges and a TM-helix bearing this feature would presumably be energetically disfavoured.

To identify possible electrostatic protein–membrane interactions we compared the electrostatic surfaces of NDH-2 (membrane binding) and 2NPX (soluble). 2NPX has a net charge of −19 while NDH-2 has a positive net charge of +6. Positively charged protein residues are generally favourable for interacting with membrane surfaces; the inner membrane of *E. coli*, for example, contains 20–25% negatively charged lipids [39]. Comparing the NADH-peroxidase structure and the model for NDH-2 reveals a four residue patch of solely positively charged amino acids in NDH-2 (Arg29–Lys32). Three of these residues are absent in the NADH-peroxidase. Equivalent positive patches are present in the closest homologues to *E. coli* NDH-2. Considering the position of this insertion in combination with the location of the two predicted amphipathic C-terminal helices suggests that NDH-2, in the orientation in which it is displayed in Fig. 1, must be topping the membrane. In this arrangement the adenosine part of NADH is pointing towards the cytosol and the isoalloxazine ring of FAD is close to the membrane. The potential ubiquinone binding site (see Section 3.3) is located between the FAD ring plane and the membrane. This orientation would appear optimal for electron transfer from NADH to ubiquinone and subsequent exchange with the membrane quinone pool.

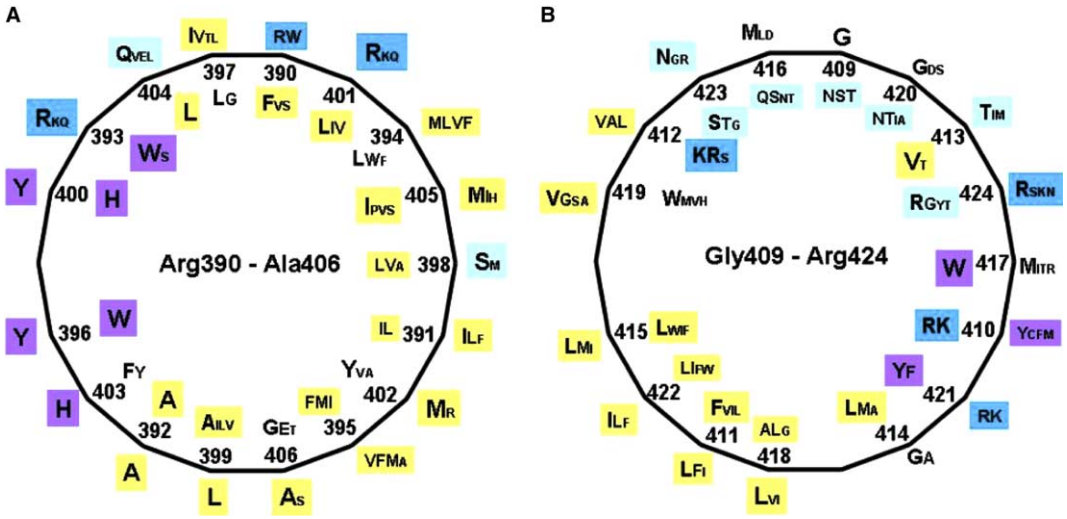

Fig. 3. Helix-wheel representations of the two predicted C-terminal helices (Panel A: Arg390–Ala406; Panel B: Gly409–Arg424) for the NDH-2 subfamily alignment (*E*-value cutoff 10^{-30}, with respect to *E. coli* NDH-2). Two distinguishable groups are treated separately; sequences belonging to the DHNA_ECOLI group are displayed on the outside of the helix wheel, sequences belonging to the YLID_BACSU group on the inside. The groups consist of 14 and 13 sequences, respectively. Different font sizes denote the number of occurrences of the respective residue in the alignment (1–2; 3–5; 6–10; >10). The colouring scheme matches physical properties of the residues at each position; blue boxes correspond to predominantly positively charged residues; light blue boxes to predominantly hydrophilic residues, yellow boxes to predominantly hydrophobic residues and violet boxes to Trp, Tyr and His, i.e. polar aromatic residues which are potentially important for membrane binding.

Two models describing the mode of interaction of NDH-2 from *E. coli* with the membrane have previously been derived from sequence studies [34,40,41]. Finel [40] suggested that binding between membrane and protein is accomplished by amphipathic interactions with residues Leu242 to Thr247. In our model most of these residues are within 5 Å of the adenosine moiety of NADH. Since in the reaction cycle NAD^+ is replaced by NADH from the cytosol they are much more likely to be in contact with the cytosol than the membrane. Contrary to Finel, Rapisarda et al. [34] postulated two C-terminal transmembrane helices acting as membrane anchors for NDH-2 based on TM-predictions by PHDTM and HMMTOP. However, the lengths of the suggested TM-helices, 11 and 13 residues respectively, seem too short for spanning the entire membrane. Therefore, we propose our model here as a more plausible approximation of the interaction between NDH-2 and membrane.

3.5. NDH-2 from E. coli in relation to alternative NADH:ubiquinone oxidoreductases from fungi, plants and bacteria

Alternative NADH:quinone oxidoreductases are found in bacteria and in mitochondria of fungi and plants. While most bacteria seem to have only one, two NDH-2 enzymes co-exist in some eukaryotic species facing either the mitochondrial matrix, or the cytoplasm. From sequence alignments these NDH-2 enzymes appear to be paralogs resulting from gene duplication events after specification (see [2] for discussion). Further in contrast to bacterial NDH-2, most eukaryotic NDH-2 have an N-terminal extension for which the structural model of *E. coli* NDH-2 obviously cannot account. Nonetheless features derived from the modelled core structure are likely to be common in all NDH-2. Specifically, most of the residues involved in FAD and NADH binding are within conserved sequence stretches, therefore we expect that the binding sites of *E. coli* NDH-2 will be useful models for the FAD and NADH binding sites in general. Of the residues forming side-chain hydrogen bonds with FAD or NADH (see Fig. 2) Thr180, Glu214 (Gln or Asp in some species) and Asp314 are conserved amongst almost all species. Asp39 which is conserved in most bacterial NDH-2 is matched by a Ser residue in most eukaryotic NDH-2, while Asn41 and His361 show less overall conservation. Within the proposed ubiquinone binding site His51 (Tyr in some species) and Glu52 (or Gln in some species) are present in bacterial NDH-2. In eukaryotic NDH-2 the corresponding residues are Pro and Ser, suggesting that the Ser residue may form a hydrogen bond to ubiquinone. By contrast, potentially Ca^{2+}-binding insertions have been found only in the potato *Solanum tuberosum* and the fungus *Neurospora crassa* NDH-2 sequences, and proposed to be involved in membrane association [2,42]. The corresponding insertion site in the *E. coli* NDH-2 model could allow a hypothetical Ca^{2+}-binding domain consisting of two EF-hands to interact with the membrane. While the same would not hold true for many other positions in the model, the absence of definitive template positions for the linker residues in between the domains means that alternative locations, farther away from the membrane, are equally plausible from a modeller's perspective. Finally, the proposal of a NDH-2 membrane interaction via two C-terminal amphiphilic helices is based on the conservation of physical properties in the alignment of bacterial sequences but inspection of this region in eukaryotic sequences suggests that it should apply generally to all NDH-2.

4. Availability

Atomic coordinates for *E. coli* NDH-2 are publicly available via the PDB as a theoretical model (PDB: 1OZK).

Acknowledgement: R.S. thanks the Deutsche Forschungsgemeinschaft (Schm-1588) for a postdoctoral research fellowship and the Edinburgh Protein Interaction Centre (EPIC) for computational facilities.

Appendix A. Supplementary data

Supplementary data associated with this article can be found, in the online version at doi:10.1016/j.febslet.2004.10.093.

References

[1] Lo Conte, L., Ailey, B., Hubbard, T.J.P., Brenner, S.E., Murzin, A.G. and Chothia, C. (2000) Nucl. Acids Res. 28, 257–259.
[2] Kerscher, S.J. (2000) Biochim. Biophys. Acta 1459, 274–283.
[3] Unden, G. and Bongaerts, J. (1997) Biochim. Biophys. Acta 1320, 217–234.
[4] Kelley, L.A., MacCallum, R.M. and Sternberg, M.J.E. (2000) J. Mol. Biol. 299, 499–520.
[5] Karplus, K., Barrett, C. and Hughey, R. (1998) Bioinformatics 14, 846–856.
[6] Altschul, S.F., Madden, T.L., Schaffer, A.A., Zhang, J.H., Zhang, Z., Miller, W. and Lipman, D.J. (1997) Nucl. Acids Res. 25, 3389–3402.
[7] Combet, C., Blanchet, C., Geourjon, C. and Deleage, G. (2000) Trends Biochem. Sci. 25, 147–150.
[8] Notredame, C., Higgins, D.G. and Heringa, J. (2000) J. Mol. Biol. 302, 205–217.
[9] Shindyalov, I.N. and Bourne, P.E. (1998) Prot. Eng. 11, 739–747.
[10] Stehle, T. and Schulz, G.E. (1992) J. Mol. Biol. 224, 1127–1141.
[11] Sali, A. and Blundell, T.L. (1993) J. Mol. Biol. 234, 779–815.
[12] Rodriguez, R., Chinea, G., Lopez, N., Pons, T. and Vriend, G. (1998) Bioinformatics 14, 523–528.
[13] Bower, M.J., Cohen, F.E. and Dunbrack, R.L. (1997) J. Mol. Biol. 267, 1268–1282.
[14] Krogh, A., Larsson, B., von Heijne, G. and Sonnhammer, E.L.L. (2001) J. Mol. Biol. 305, 567–580.
[15] Rost, B., Casadio, R., Fariselli, P. and Sander, C. (1995) Prot. Sci. 4, 521–533.
[16] Tusnady, G.E. and Simon, I. (2001) Bioinformatics 17, 849–850.
[17] Hofmann, K. and Stoffel, W. (1993) Biol. Chem. Hoppe-Seyler 374, 166.
[18] Cserzo, M., Wallin, E., Simon, I., vonHeijne, G. and Elofsson, A. (1997) Prot. Eng. 10, 673–676.
[19] Pasquier, C., Promponas, V.J., Palaios, G.A., Hamodrakas, J.S. and Hamodrakas, S.J. (1999) Prot. Eng. 12, 381–385.
[20] Deber, C.M., Wang, C., Liu, L.P., Prior, A.S., Agrawal, S., Muskat, B.L. and Cuticchia, A.J. (2001) Prot. Sci. 10, 212–219.
[21] Milpetz, F., Argos, P. and Persson, B. (1995) Trends Biochem. Sci. 20, 204–205.
[22] Nakai, K. and Kanehisa, M. (1992) Genomics 14, 897–911.
[23] Hirokawa, T., Boon-Chieng, S. and Mitaku, S. (1998) Bioinformatics 14, 378–379.
[24] Nicholls, A., Sharp, K.A. and Honig, B. (1991) Proteins 11, 281–296.
[25] Sobolev, V., Sorokine, A., Prilusky, J., Abola, E.E. and Edelman, M. (1999) Bioinformatics 15, 327–332.
[26] Bellamacina, C.R. (1996) Faseb J. 10, 1257–1269.
[27] Eggink, G., Engel, H., Vriend, G., Terpstra, P. and Witholt, B. (1990) J. Mol. Biol. 212, 135–142.
[28] Kuriyan, J., Krishna, T.S.R., Wong, L., Guenther, B., Pahler, A., Williams, C.H. and Model, P. (1991) Nature 352, 172–174.
[29] Fisher, N. and Rich, P.R. (2000) J. Mol. Biol. 296, 1153–1162.
[30] Schmid, R., Gerloff, D.L., in preparation.
[31] Faig, M., Bianchet, M.A., Chen, S., Winski, D., Ross, D. and Amzel, L.M. (2000) Proc. Nat. Acad. Sci. USA 97, 3177–3182.
[32] de Vries, S., van Witzenburg, R., Grivell, L.A. and Marres, C.A.M. (1992) Eur. J. Biochem. 203, 587–592.
[33] Rapisarda, V.A., Montelongo, L.R., Farias, R.N. and Massa, E.M. (1999) Arch. Biochem. Biophys. 370, 143–150.
[34] Rapisarda, V.A., Chehin, R.N., Rivas, J.D., Rodriguez-Montelongo, L., Farias, R.N. and Massa, E.M. (2002) Arch. Biochem. Biophys. 405, 87–94.
[35] Nilsson, J., Persson, B. and von Heijne, G. (2000) Febs Lett. 486, 267–269.
[36] Moller, S., Croning, M.D.R. and Apweiler, R. (2001) Bioinformatics 17, 646–653.
[37] Benner, S.A., Cannarozzi, G., Gerloff, D., Turcotte, M. and Chelvanayagam, G. (1997) Chem. Rev. 97, 2725–2843.
[38] Reithmeier, R.A.F. (1995) Cur. Opin. Struct. Biol. 5, 491–500.
[39] Opekarova, M. and Tanner, W. (2003) Biochim. Biophys. Acta 1610, 11–22.
[40] Finel, M. (1996) Febs Lett. 393, 81–85.
[41] Bjorklof, K., Zickermann, V. and Finel, M. (2000) FEBS Lett. 467, 105–110.
[42] Rasmusson, A.G., Svensson, A.S., Knoop, V., Grohmann, L. and Brennicke, A. (1999) Plant J. 20, 79–87.
[43] Kraulis, P.J. (1991) J. Appl. Cryst. 24, 946–950.
[44] Merritt, E.A. and Bacon, D.J. (1997) Macromol. Crystallogr. B 277, 505–524.
[45] Westhead, D.R., Slidel, T.W.F., Flores, T.P.J. and Thornton, J.M. (1999) Prot. Sci. 8, 897–904.